

## Atomic and electronic structures of oxygen on Si(100) surfaces: Metastable adsorption sites

Yoshiyuki Miyamoto and Atsushi Oshiyama

*Fundamental Research Laboratories, NEC Corporation, 34 Miyukigaoka, Tsukuba-shi, Ibaraki-ken 305, Japan*

(Received 18 January 1990)

We have explored the mechanisms of oxygen adsorption on Si(100) reconstructed surfaces by first-principles total-energy band-structure and force calculations for slab geometries within the local-density approximation. The oxygen and the surface Si atoms are fully relaxed, according to the calculated forces acting on the atoms, toward the total-energy-optimized configurations. We have found three (*meta*)stable adsorption sites for the oxygen atom. Upon oxygen adsorption, the original dimer is *preserved*, *twisted*, or *decomposed*, depending on which site the oxygen is adsorbed. The adsorption energy for the (*meta*)stable configurations are so large that an  $O_2$  molecule dissociates exothermically on the Si surfaces. In fact, the  $O_2$  molecule is shown to dissociate on the Si dimer due to electron transfer from the Si dangling bond to the antibonding orbital of the  $O_2$  molecule. Comparison of the calculated valence density of states and vibrational frequency with existing experimental data indicates that the most stable atomic adsorption site is realized in typical experimental conditions. We propose, however, that other metastable configurations manifest themselves at early stages of the oxygen adsorption.

### I. INTRODUCTION

Atomic and molecular adsorption on semiconductor surfaces is a fundamental phenomenon in condensed-matter physics and surface science. In particular, oxygen adsorption on Si surfaces is important, since it is an initial stage of oxidation of the materials, on the one hand, and its microscopic understanding provides a basis of silicon technology, on the other. Many experimental and theoretical works<sup>1-13</sup> have been done to reveal atomic and electronic structures of oxygen on Si surfaces. High-resolution electron-electron-loss spectroscopy (HREELS) on Si surfaces upon oxygen exposure provides energy spectra of local vibrational modes related to adsorbed oxygen atoms.<sup>3-5,11</sup> Although the data scatter to some extent, the bond configurations between the adsorbed oxygen atom and the substrate Si atoms have been deduced by comparing the measured vibrational energies with those of isolated molecules. The HREELS measurements infer the existence of the Si—O—Si bond at the early stage of oxidation on both Si(100) and (111) surfaces. The Si—O—Si bond has been also proposed from the surface extended x-ray-absorption fine structure (SEXAFS) measurement.<sup>13</sup> The photoemission spectroscopies<sup>1,12</sup> provide information on the electronic structures of the oxygen-adsorbed Si surface. One of the characteristic features is the appearance of three new peaks in the original peaks in the original Si valence band upon oxygen adsorption, although the exact locations of the peaks are quite different among the experimental situations. The possibility of molecular adsorption for oxygen on Si(111) surfaces has been also suggested from the photoemission and near-edge x-ray-absorption data,<sup>14</sup> whereas only the atomic adsorption has been reported for Si(100) surfaces.

The empirical tight-binding band calculation has been performed by Ciraci *et al.*<sup>8</sup> They discuss plausible adsorption sites for oxygen through comparison between the calculated density of states and photoemission data. On the other hand, the total-energy calculation done by Batra *et al.*<sup>10</sup> for small clusters that mimic the oxygen-adsorbed Si(100) surfaces indicates that a hollow bridge site is most favorable energetically for the oxygen adsorption.

Despite the considerable efforts described above, microscopic understanding of oxygen adsorption on the Si surface is not satisfactory: Knowledge of the mechanism of dissociation of the  $O_2$  molecule, of the energetics for the adsorbed oxygen atom, of the relaxation of the Si atoms upon the oxygen adsorption, and of the relation between the atomic and electronic structures of the oxygen-adsorbed Si surface still remains insufficient. We have thus performed first-principles total-energy band-structure calculations for the oxygen on the Si(100) surface within the local-density approximation (LDA) using *ab initio* norm-conserving nonlocal pseudopotentials. We have found several (*meta*)stable atomic configurations for oxygen adsorption and the consequent displacements of the surface Si atoms. In this paper we present the detailed results for the oxygen dissociation and adsorption on the Si(100) surface. Experimental data are discussed in light of the calculated density of states and the local vibrational frequency.

In Sec. II the method of the present calculation is explained. Calculated results are presented in Sec. III and in Sec. IV summary and discussion are given.

### II. CALCULATION

The calculation has been done for the slab geometry within the local-density approximation (LDA) using

norm-conserving nonlocal pseudopotentials.<sup>15,16</sup> The total energy  $E_t$  of a many-body system is thus expressed as a function of valence-electron density  $\rho$ ,<sup>17</sup>

$$E_t = T[\rho] + \int V_{lo}(r)\rho(r)dr + \sum_i^{\text{occ}} \int \int \psi_i(r')V_{nl}(r',r)\psi_i(r)dr' dr + \int \frac{\rho(r')\rho(r)}{|r-r'|}dr' dr + E_{xc}[\rho] + \frac{1}{2} \sum \frac{Z_I Z_J}{|R_I - R_J|}, \quad (1)$$

where

$$\rho(r) = \sum_i^{\text{occ}} |\psi_i|^2. \quad (2)$$

Here  $T[\rho]$  indicates a kinetic energy, and  $V_{lo}$  and  $V_{nl}$  indicate the local and nonlocal parts of the pseudopotentials, respectively. Electrostatic energies between valence electrons and between nuclei are written in the fourth and in the last term. As for the exchange-correlation energy  $E_{xc}[\rho]$  of valence electrons we have used the Perdew-Zunger analytic form<sup>18</sup> which has been fitted to the numerical results by Ceperley and Alder.<sup>19</sup>

One electron wave function  $\psi_i$  is obtained by solving the Kohn-Sham equation

$$H\psi_i = \epsilon_i \psi_i, \quad (3)$$

where  $H$  is an effective Hamiltonian given by

$$H = -\nabla^2 + V_{lo} + V_{nl} + \int \frac{\rho(r')}{|r-r'|}dr' + \frac{\delta E_{xc}[\rho]}{\delta \rho}. \quad (4)$$

When the plane-wave basis set is used for the expansion of the wave function, a huge number of plane waves is required to obtain the well-converged total energy and then stable atomic geometries for the oxygen-adsorbed Si(100) surface, because of the large volume of the unit cell and the rather compact orbitals of the oxygen valence electrons. In this work we therefore adopt a Gaussian-orbitals basis set to reduce the size of the basis set. The exponents are determined by fitting the numerically obtained orbitals from all electron calculations of each atom, and then minimizing the total energy of solids. In this calculation three exponents are used for Si  $s$ , O  $s$  and  $p$  orbitals, and two exponents for Si  $p$  orbitals: in atomic units 0.18, 0.44, and 1.30 for Si  $s$ ; 0.18, 0.55 for Si  $p$ ; 0.2812, 1.0996, and 4.4573 for O  $s$ ; and 0.2213, 1.0694, and 5.5000 for O  $p$ .

Calculation of the forces acting on the atoms is inevitable to find stable geometries efficiently. The forces are obtained as negative gradients of the total energy with respect to the atomic coordinations  $\tau$ ,<sup>20</sup>

$$F\tau = -\sum_i^{\text{occ}} \left\langle \psi_i \left| \frac{V_{lo}}{\delta \tau} + \frac{\delta V_{nl}}{\delta \tau} \right| \psi_i \right\rangle + \sum_I \frac{Z_I \tau Z_I}{|\tau - R_I|^3} (\tau - R_I) - 2 \text{Re} \sum_i^{\text{occ}} \left\langle \frac{\delta \psi_i}{\delta \tau} \left| H - \epsilon_i \right| \psi_i \right\rangle. \quad (5)$$

The first and the second terms are Hellmann-Feynman forces, and the third is a correction term.

Real adsorbed surfaces are simulated by the slabs that contain typically four or eight layers of Si plus sufficiently thick vacuum layers. Examination of sufficient thickness of the slabs is described in Sec. III. Oxygen atoms are placed on the top and bottom of the slabs so that the  $C_2$  symmetry is preserved. In the total-energy band-structure and force calculation, we use eight  $k$  points for the integration over Brillouin zone. The 14 real-space mesh points per bond length in  $[011]$  and  $[0\bar{1}1]$  directions and the ten points in  $[100]$  direction are found to be enough to express the wave functions in the fast Fourier transformation. The optimization of the atomic geometry is performed with the quasi-Newton-Raphson method. During the optimization we keep equivalent geometries in both sides of a slab.

The above ingredients in the calculation can reproduce the following key results previously established: First, calculated lattice constant and bulk modulus for the Si crystal is 5.44 Å and 0.9 Mbar, respectively. Second, a calculated lattice constant for the  $\alpha$  quartz agrees with an experimental value in a difference of 2%, and the consequent cohesive energy 1.68 Ry per SiO<sub>2</sub> agrees both with an experimental value and the well-converged plane-wave basis-set results.<sup>21</sup> Finally, a calculated energy gain of the dimerized Si(100)2×1 surface is 1.6 eV per dimer, which agrees reasonably with the plane-wave basis-set result, 1.5 eV.<sup>22</sup>

### III. RESULTS

The first-principles calculation described in Sec. II provides us with fruitful results. In Sec. III A mechanisms of dissociation of an oxygen molecule on the Si(100) surface are discussed on the basis of the present total-energy force calculation. In Sec. III B several (meta)stable geometries that we have found for an adsorbed oxygen atom are presented. In Sec. III C the calculated density of states for these (meta)stable geometries is presented and compared with the ultraviolet photoemission spectroscopy (UPS) data. The vibrational frequency corresponding to each (meta)stable geometry is calculated and is found to agree reasonably with the HREELS data in Sec. III D.

#### A. Dissociation of oxygen molecule

We have performed the total-energy and the force calculation for an adsorbed oxygen molecule on the Si(100) surface. We have found that dissociation of an oxygen molecule occurs when the molecule approaches above the dimer with its molecular axis normal to the surface. At first we adopt a slab consisting of four-layers of Si and eight-layers of vacuum. In the lateral direction the boundary condition corresponding to the 2×1 period is imposed. The total-energy minimized Si(100)2×1 surface with symmetric dimers has been obtained and is regarded as the clean Si(100) surface. Two oxygen molecules are then placed on equivalent sites on both sides of the slab with the molecular axis normal to the surfaces.

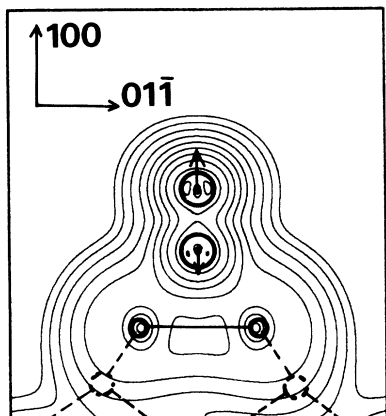


FIG. 1. Dissociation of the oxygen molecule on the dimerized Si(100) surface. The two arrows indicate the calculated forces acting on the oxygen atoms (0.137 Ry/a.u. on the upper oxygen and 0.085 Ry/a.u. on the lower oxygen). The contour map shows a valence charge density on the (011) plane. The maximum value of the contour is 0.518 electron/(a.u.)<sup>3</sup>.

It is found that the eight-layer vacuum is sufficient to eliminate the interaction between the two oxygen molecules via the vacuum region. In Fig. 1 dissociation of an oxygen molecule is demonstrated. It is shown that the forces act on the oxygen atoms so as to make the molecule dissociate. This is explained by electron transfer from the Si dangling bonds to the antibonding orbital of the molecule (see the contour map in Fig. 1). Further, we have performed the total-energy calculation for an isolated oxygen molecule,<sup>23</sup> and the obtained cohesive energy of the molecule is 5.15 eV per atom. This value is considerably smaller than the adsorption energy (more than 7 eV, as is presented in Sec. III B) of an oxygen atom on the Si(100) surface. Therefore, atomic rather than molecular adsorption of the oxygen on the Si(100) surface is energetically favorable.

### B. Geometry optimization for adsorbed oxygen atom

Since the atomic adsorption is energetically favorable compared with the molecular adsorption, the next step is the determination of adsorption sites for an oxygen atom. We have searched (meta)stable adsorption sites in the whole range over the Si(100) surface. We place an oxygen atom at one site on the surface and then perform geometry optimization according to the calculated force acting on each atom. We next choose another site and repeat this procedure to reach (meta)stable atomic configurations. In this way we have examined several adsorption sites on the Si dimer, between the nearest-neighbor dimers and between the row of the dimers, which almost cover the Si(100) surface. The geometry optimization for each adsorption site has been performed as follows. Since we prefer to keep  $C_2$  symmetry of the slab, two oxygen atoms are placed at each adsorption site of both sides of the slab. At the first step, only the oxygen atoms are optimized until forces on them are reduced less than 0.05 Ry/a.u., using the slab consisting of four-

layers of Si and four-layers of vacuum, with the lateral periodic boundary condition corresponding to the  $2 \times 1$  period. In the next step the geometry optimizations for the oxygen atoms and the surface Si atoms are performed with other Si atoms being fixed at the Si lattice sites. The optimization is continued until the force on each atom is reduced to less than 0.02 Ry/a.u. We then increase the thickness of the Si slab from four layers to eight layers and perform the force calculation again. In usual cases the calculated forces still remain less than 0.02 Ry/a.u.,<sup>24</sup>

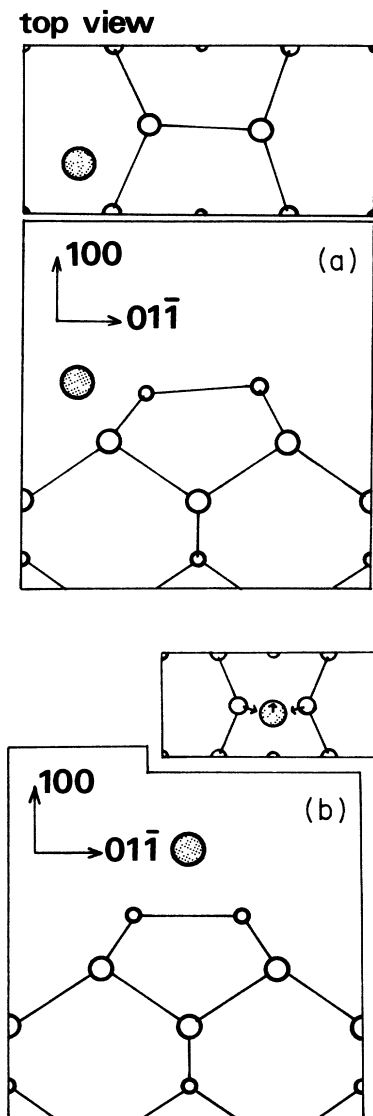


FIG. 2. (a) Metastable atomic geometry of adsorbed oxygen shown on the (011) plane. Dotted and open circles indicate the oxygen atoms and silicon atoms, respectively. The oxygen atom is 0.7 Å apart from the (011) plane and the dimer is buckled and twisted (see the upper panel viewed from the [100] direction). (b) Metastable atomic geometry of adsorbed oxygen. The oxygen atom shares the same (011) plane with the dimer. This atomic geometry is stable against the displacement of the oxygen atom away from the (011) plane (see the forces in upper panel viewed from the [100] direction).

and the existence of a (meta)stable atomic configuration is thus confirmed.

We have found two metastable geometries that still preserve the dimer structure of the Si(100)2×1 surface. These structures are shown in Figs. 2(a) and 2(b). In the geometry shown in Fig. 2(a), an oxygen atom is located 0.7 Å apart from the (011) plane containing the original dimer [see the top view in Fig. 2(a)]. The dimer is in turn tilted and twisted upon oxygen adsorption. The calculated bond length between the oxygen atom and the nearest Si atom is 1.9 Å. Another geometry that we have found is shown in Fig. 2(b). The oxygen atom is located above the dimer and it shares the (011) plane with the Si atoms of the dimer. The dimer is slightly distorted to reduce its bond length between the two Si atoms. The bond length is Si—O is also 1.9 Å and the bond angle of Si—O—Si is 74.4°. When the oxygen atom is displaced from the (011) plane, the calculated force acts on the oxygen atom back to the plane [see the upper panel of Fig. 2(b)]—namely, this geometry is stable against the motion of the oxygen atom normal to the (011) plane. The calculated binding energies of the oxygen atom in the geometries shown in Figs. 2(a) and 2(b) are 6.8 and 7.6 eV, respectively. We have searched other oxygen adsorption sites between the two rows of the dimers. It is found that the total energies for the configurations are higher than the corresponding values for the metastable geometries in Figs. 2(a) and 2(b) by about 5 eV.

The most stable geometry, shown in Fig. 3, has been achieved when the oxygen atom intervenes between the dimer from the position shown in Fig. 2(b). The binding energy of the oxygen atom for the most stable geometry is 8.2 eV. The Si dimer has been decomposed and a new Si—O—Si bridge bond is formed. The bond length of Si—O is 1.68 Å and the Si—O—Si angle is 174°. Again we have confirmed that this geometry is stable against the

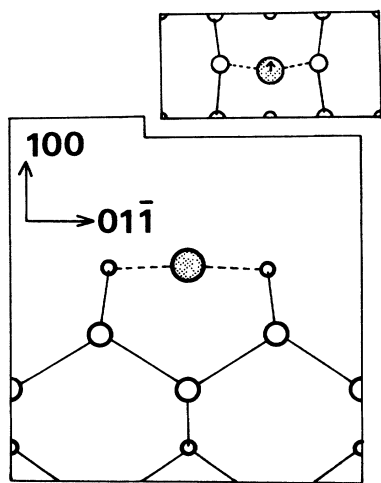


FIG. 3. Stable atomic geometry of adsorbed oxygen atom on Si(100) surface. The oxygen atom intervenes between the Si atoms of the original dimer. This atomic geometry is stable against the displacement of the oxygen atom away from the (011) plane (see the forces in upper panel viewed from the [100] direction).

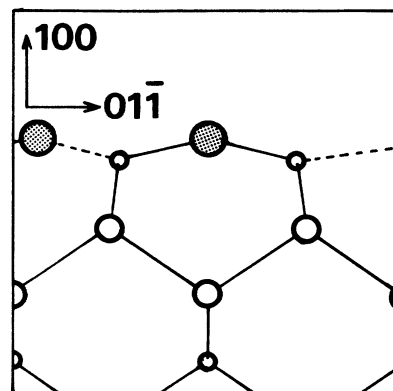


FIG. 4. Stable atomic geometry for the new oxygen atoms on the Si(100) surface. The oxygen atoms and the top-layer Si atoms are in the (011) plane.

displacement of the oxygen atom apart from the (011) plane.

The geometry optimizations for an adsorbed oxygen atom have been extended to the cases of higher coverage. We have placed another oxygen atom on the oxygen-adsorbed surface shown in Fig. 3 and performed the total-energy optimization. It is found that in the optimized geometry the added oxygen atom shares the (011) plane with the previous Si—O—Si (see Fig. 4). The stability of the geometry against the displacement of the oxygen atom from the (011) plane has been confirmed in the same manner as before. We have compared the binding

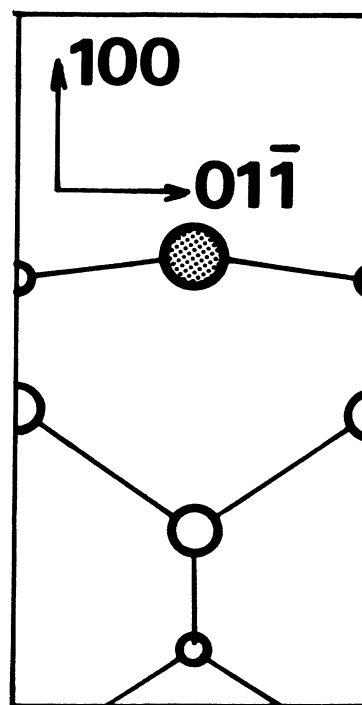


FIG. 5. Hollow bridge geometry for the adsorbed oxygen atom on the Si(100) ideal surface.

energy per oxygen atom of this geometry with that of the previously proposed geometry<sup>10</sup> in which the oxygen atom is located on a hollow bridge site of the Si(100) ideal surface (see Fig. 5). The calculated binding energy per oxygen atom for Fig. 4 is 7.81 eV, whereas that for Fig. 5 is 7.88 eV.<sup>25</sup> This slight total-energy difference indicates that the transition in atomic configurations between these geometries occurs easily at finite temperature. This result is consistent with the experimental work<sup>13</sup> that at an early stage of the oxidation of the Si(100) surface the  $2 \times 1$  ordered structure disappears at room temperature.

### C. Density of states and comparison with ultraviolet photoelectron spectroscopy (UPS) measurement

Comparison of the calculated valence-band density of states (DOS) for the (meta)stable geometries with the UPS experimental data is important to examine whether the metastability manifests itself in photoemission spectra. We have found that the DOS of the stable geometries in Figs. 3, 4, and 5, in which the Si—O—Si bridge bonds are formed, reasonably agree with the UPS data.<sup>1,12</sup>

Ibach and Rowe<sup>1</sup> have shown the appearance of three new characteristic peaks in the valence-band region upon oxygen adsorption with monolayer coverage. Hollinger and Himpsel<sup>12</sup> have also found the appearance of the three peaks when the oxygen is adsorbed with one-half monolayer coverage and then the surface is annealed at 700°C. The experimental data on the energy separation between the three peaks are scattered to some extent: The separation is 2.5 or 3.3 eV for the first and the second (in the order of increasing binding energy) peaks, and is 3.3 or 4.0 eV for the second and the third peaks.

The DOS has been calculated for the several (meta)stable geometries that we have found. The results are shown in Figs. 6(a), 6(b), and 6(c), which correspond to the geometries in Figs. 2(a), 2(b), and Fig. 3, respectively. And the calculated DOS of the optimized Si(100) $2 \times 1$  surface is also shown in Fig. 6(d) to clarify the effect of oxygen adsorption. In these calculations the energy resolution is taken as 0.4 eV. By comparing Figs. 6(a), 6(b), and 6(c) with Fig. 6(d), one can easily notice the appearance of a peak about 20 eV below the Fermi level upon oxygen adsorption. It comes from the O 2s level and is out of range in the UPS measurements. Further, it is found that three characteristic peaks appear only in the calculated DOS in Fig. 6(c) corresponding to the most stable geometry shown in Fig. 3. The calculated energy separations between the peaks are 2.0 eV for the first and the second peaks and 4.0 eV for the second and the third peaks, respectively. These results reasonably agree with the experimental data. The DOS for the geometries shown in Figs. 4 and 5 has also been calculated (not shown here). In that case the three peaks still appear and they are shifted upward because the increase of the oxygen coverage causes more electron transfer to the oxygen layer.

From our calculations it is concluded that the characteristic three peaks in the UPS data are related to the Si—O—Si bridge bonds formed on the surface and the

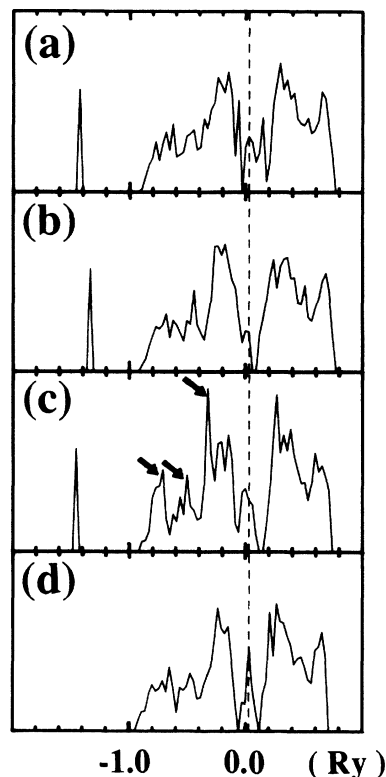


FIG. 6. The calculated DOS for the several (meta)stable geometries. The dotted lines indicate the position of the Fermi level. The DOS curves in (a), (b), and (c) correspond to the atomic geometries in Figs. 2(a), 2(b), and 3, respectively. The DOS curve in (d) is the DOS of the clean surface with the symmetric dimers. The arrows in (c) indicate the characteristic peaks that agree with the experimental works (Refs. 1 and 12).

peak positions are sensitive to the oxygen coverage. Other bonding configurations are not likely to be detected in the typical experimental conditions.

### D. Local vibration frequency and comparison with the HREELS measurement

Local vibrational modes are other fingerprints of the (meta)stable geometries. We have compared the calculated vibrational energies for the geometries shown in Figs. 2(b) and 3 with the HREELS measurements.<sup>11</sup> According to the HREELS measurements,<sup>5,11</sup> the existence of the symmetric and antisymmetric stretching modes of the Si—O—Si unit in the oxygen-adsorbed Si(100) surface have been reported. In the experimental conditions the dipole scattering by the adsorbed oxygen is a dominant scattering mechanism for incident electrons. The vibrational motion normal to the surface is thus observed.<sup>26</sup> Considering the vibrational mode normal to the surface in the geometries obtained by the present calculations, it is noticed that only the symmetric stretching mode in Figs. 2(b) and 3 and the symmetric and antisymmetric

stretching mode in Fig. 2(a) are able to be detected. The binding energy for the geometry in Fig. 2(a) is somewhat smaller than those for the other geometries. Thus we have calculated only the vibrational energies of symmetric stretching modes in the geometries shown in Figs. 2(b) and 3. To perform the calculations, we have used the slab consisting of four layers of Si and four layers of vacuum and have treated the Si—O—Si unit as an isolated molecule, i.e., we have fixed other Si atoms at their lattice sites. The calculated total energies for several atomic positions have been fitted to a parabolic form as a function of atomic displacements.

According to the HREELS measurements, the peak positions that related to the symmetric stretching mode vary from 91 to 98 meV with changing oxygen coverage.<sup>11</sup> In the present work, the calculated vibrational energies of the symmetric stretching modes in Figs. 2(b) and 3 are 80 and 81 meV, respectively. These are in reasonable agreement with the experimental data. In general, the vibrational energies of the localized modes are determined by the local bond configurations and the corresponding force constants.<sup>27</sup> If the force constants of the Si—O bond are almost equal in the two geometries, Figs. 2(b) and 3, the vibrational energy in the geometry in Fig. 2(b) should be higher than the corresponding value in Fig. 3. But, in fact, the covalent bond of the original dimer still remains in Fig. 2(b), so that the force constant of the Si—O in Fig. 2(b) is weaker than that in Fig. 3. This results in the vibrational energies of these two geometries being almost equal.

From our calculations, it is concluded that the geometries shown in Figs. 2(b) and 3 are realized under the HREELS measurements but that the two geometries are indistinguishable by the comparison between the present calculations with the HREELS experiments.

#### IV. DISCUSSION AND SUMMARY

Calculated DOS and vibrational energy of the oxygen atom for the most stable geometry in Fig. 3 is consistent with both UPS (Refs. 1 and 12) and HREELS (Refs. 3, 5, and 11) measurements. We have thus concluded that the most stable geometry is realized in these experimental situations. Further, we propose here that the metastable geometries that were obtained by the present calculations can be realized under a well-controlled experimental situation at low coverage or at low temperature. Recently, the existence of the  $2 \times 1$  periodicity in a  $\text{SiO}_2/\text{Si}(100)$  interface formed by a molecular-beam deposition has been found by grazing incidence x-ray diffraction measurement.<sup>28</sup> These data suggest the manifestation of the metastable geometries that we have found and their preservation at the interface.

In summary, we have performed the total-energy band-structure calculations to reveal the mechanism of dissociation and adsorption of oxygen on  $\text{Si}(100)$  reconstructed surface. It is found that dissociation of an oxygen molecule occurs exothermically and is explained by electron transfer from the Si dangling bond to the antibonding orbital of the molecule. Several metastable atomic geometries for an adsorbed oxygen atom have also been discovered. The metastability is a consequence of flexibility of bond configurations of the Si and O atoms.

#### ACKNOWLEDGMENTS

We thank A. Ishitani, T. Tatsumi, J. Mizuki, I. Hiro-sawa, and H. Tsuda for valuable discussions. We have also benefited from conversations with N. Shima and M. Saito on the numerical calculation technique. These computations have been performed on an NEC SX-2 supercomputer system.

<sup>1</sup>H. Ibach and J. E. Rowe, *Phys. Rev. B* **10**, 710 (1974), and references therein.

<sup>2</sup>R. Ludeke and A. Koma, *Phys. Rev. Lett.* **34**, 1170 (1975).

<sup>3</sup>S. Fujiwara, M. Ogata, and M. Nishijima, *Solid State Commun.* **21**, 895 (1977).

<sup>4</sup>C. M. Garner, I. Lindau, C. Y. Su, P. Pianetta, and W. E. Spicer, *Phys. Rev. B* **19**, 3944 (1979).

<sup>5</sup>H. Ibach, H. D. Bruchmann, and W. Wagner, *Appl. Phys. A* **29**, 113 (1982).

<sup>6</sup>W. A. Goddard III, A. Redondo, and T. C. McGill, *Solid State Commun.* **18**, 981 (1976).

<sup>7</sup>M. Chen, I. P. Batra, and C. R. Brundle, *J. Vac. Sci. Technol.* **16**, 1216 (1979).

<sup>8</sup>S. Ciraci, S. Ellialtioglu, and S. Erkoç, *Phys. Rev. B* **26**, 5716 (1982).

<sup>9</sup>V. Barone, F. Lelj, N. Rosso, and M. Toscano, *Phys. Rev. Lett.* **113A**, 321 (1985); *Surf. Sci.* **162**, 230 (1985).

<sup>10</sup>I. P. Batra, P. S. Bagus, and K. Hermann, *Phys. Rev. Lett.* **52**, 384 (1984).

<sup>11</sup>J. A. Schaefer, F. Stucki, D. J. Francel, W. Gopel, and G. J. Lapeyre, *J. Vac. Sci. Technol. B* **2**, 359 (1984); J. A. Schaefer and W. Gopel, *Surf. Sci.* **155**, 535 (1985).

<sup>12</sup>G. Hollinger and F. J. Himpsel, *Phys. Rev. B* **28**, 3651 (1983);

*J. Vac. Sci. Technol. A* **1**, 640 (1983).

<sup>13</sup>L. Incoccia, A. Balerna, S. Cramm, C. Kunz, F. Senf, and I. Storjohann, *Surf. Sci.* **189/190**, 453 (1987).

<sup>14</sup>U. Höfer, P. Morgen, W. Wurth, and E. Umbach, *Phys. Rev. Lett.* **55**, 2979 (1985); U. Höfer, A. Puschmann, D. Coulman, and E. Umbach, *Surf. Sci.* **211/212**, 948 (1989).

<sup>15</sup>D. R. Hamann, M. Schlüter, and C. Chang, *Phys. Rev. Lett.* **43**, 1494 (1982); G. B. Bachelet, D. R. Hamann, and M. Schlüter, *Phys. Rev. B* **26**, 4199 (1982).

<sup>16</sup>A. Oshiyama and M. Saito, *J. Phys. Soc. Jpn.* **56**, 2104 (1987).

<sup>17</sup>See, for a review, *Theory of the Inhomogeneous Electron Gas*, edited by S. Lundqvist and W. H. March (Plenum, New York, 1983).

<sup>18</sup>J. Perdew and A. Zunger, *Phys. Rev. B* **23**, 5048 (1981).

<sup>19</sup>D. M. Ceperley and B. J. Alder, *Phys. Rev. Lett.* **45**, 566 (1980).

<sup>20</sup>C. Satoko, *Chem. Phys. Lett.* **83**, 111 (1981); P. Bendt and A. Zunger, *Phys. Rev. Lett.* **50**, 1684 (1983).

<sup>21</sup>Y. Bar-Yam, S. T. Pantelides, and J. D. Joannopoulos, *Phys. Rev. B* **39**, 3396 (1989).

<sup>22</sup>M. T. Yin and M. L. Cohen, *Phys. Rev. B* **24**, 2303 (1981).

<sup>23</sup>We have performed the total-energy calculation for an oxygen molecule within the local-spin-density approximation. We

have used the periodic boundary condition with tetragonal unit cell in which the period is 5.45 Å in parallel direction to the molecular axis and 3.85 Å in normal directions. In the band-structure calculation 16 k points per first Brillouin zone have been used. We have obtained triplet spin state as the ground state, and the bond length which minimizes the total energy is 1.3 Å.

<sup>24</sup>Forces calculated in a four-layer Si slab show a good agreement with those in an eight-layer slab with a difference of 1%.

<sup>25</sup>Location of the oxygen atom in the hollow bridge geometry has been optimized in the present work, and the resulting geometry is slightly different from the proposed one in Ref.

10.

<sup>26</sup>See for an example, the article by D. M. Newns in *Vibrational Spectroscopy of Adsorbates*, edited by R. F. Wills (Springer-Verlag, Berlin, 1980).

<sup>27</sup>See for an example, H. Ibach and D. L. Mills, *Electron Energy Loss Spectroscopy and Surface Vibrations* (Academic, New York, 1982).

<sup>28</sup>T. Tatsumi, T. Niino, A. Sakai, and H. Hirayama, Jpn. J. Appl. Phys. (to be published); I. Hirose, K. Akimoto, T. Tatsumi, J. Mizuki, and J. Matsui, *Inst. Symposium on Defect Recognition and Image Processing for Research and Development of Semiconductors, Tokyo, 1989* [J. Cryst. Growth (to be published)].

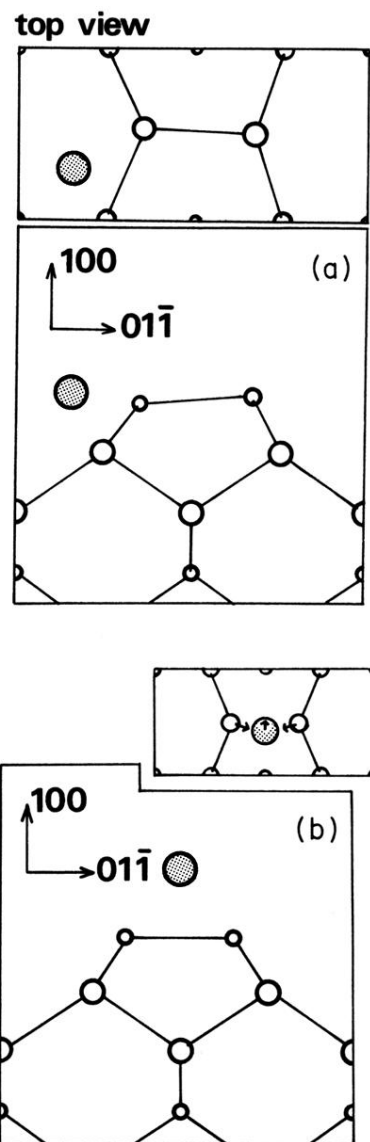


FIG. 2. (a) Metastable atomic geometry of adsorbed oxygen shown on the (011) plane. Dotted and open circles indicate the oxygen atoms and silicon atoms, respectively. The oxygen atom is 0.7 Å apart from the (011) plane and the dimer is buckled and twisted (see the upper panel viewed from the [100] direction). (b) Metastable atomic geometry of adsorbed oxygen. The oxygen atom shares the same (011) plane with the dimer. This atomic geometry is stable against the displacement of the oxygen atom away from the (011) plane (see the forces in upper panel viewed from the [100] direction).



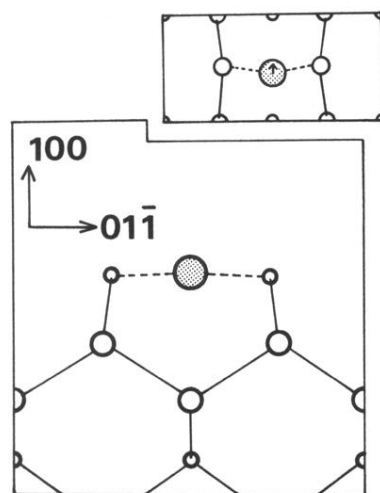


FIG. 3. Stable atomic geometry of adsorbed oxygen atom on Si(100) surface. The oxygen atom intervenes between the Si atoms of the original dimer. This atomic geometry is stable against the displacement of the oxygen atom away from the (011) plane (see the forces in upper panel viewed from the [100] direction).

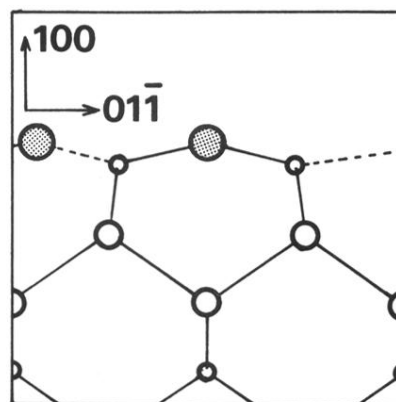


FIG. 4. Stable atomic geometry for the new oxygen atoms on the Si(100) surface. The oxygen atoms and the top-layer Si atoms are in the (011) plane.